

Fermi surface and antiferromagnetism in the Kondo lattice: an asymptotically exact solution in $d > 1$ dimensions

Seiji J. Yamamoto and Qimiao Si

Department of Physics & Astronomy, Rice University, Houston, TX 77005, USA

Interest in the heavy fermion metals has motivated us to examine the quantum phases and their Fermi surfaces within the Kondo lattice model. We demonstrate that the model is soluble asymptotically exactly in any dimension $d > 1$, when the Kondo coupling is small compared with the RKKY interaction and in the presence of antiferromagnetic ordering. We show that the Kondo coupling is exactly marginal in the renormalization group sense, establishing the stability of an ordered phase with a small Fermi surface, AF_S. Our results have implications for the global phase diagram of the heavy fermion metals, suggesting a Lifshitz transition inside the antiferromagnetic region and providing a new perspective for a Kondo-destroying antiferromagnetic quantum critical point.

PACS numbers: 71.10.Hf, 71.27.+a, 75.20.Hr, 71.28.+d

There is a growing list of materials in which quantum criticality may have a strong influence on their electronic and magnetic properties. A basic question is whether quantum criticality can be adequately described in terms of order-parameter fluctuations, or if inherently quantum effects must be incorporated. It is fortunate that the issue can be systematically studied in heavy fermion metals [1, 2]. These systems involve the Kondo effect which, via the Kondo singlet formation, is an inherently quantum property. Indeed, the discussion here has centered on whether or not the Kondo entanglement energy scale collapses at the antiferromagnetic quantum critical point (QCP). If the Kondo scale remains finite, the QCP is of the spin-density-wave (SDW) type [3, 4, 5]. If it collapses, new types of theory [6, 7, 8, 9] – such as the local quantum criticality – are needed.

To understand the QCPs, it is instructive to elucidate the proximate quantum phases. The ordered phase involved in the SDW QCP is expected to be an antiferromagnet whose Fermi surface incorporates both the conduction electrons and local moments; such a Fermi surface is called “large” and the corresponding phase is named AF_L. For a Kondo-destroying QCP, on the other hand, it must be an AF_S phase, whose Fermi surface is “small” in the sense that it encloses only the conduction electrons. Experimentally, evidence exists from dHvA measurements for the AF_S phase [10, 11] and, moreover, there are also indications [12, 13] from Hall-effect and dHvA for a direct transition from the AF_S phase to PM_L, a paramagnetic metal phase with a large Fermi surface. Theoretically, however, whether the AF_S is a stable phase of the Kondo lattice with spin-rotational invariance has not been previously established in dimensions higher than one. In this letter, we answer the question in the affirmative for the model with SU(2) spin symmetry. Our results are asymptotically exact, something that is ordinarily difficult to achieve for any correlated-electron model in more than one dimension.

We consider the Kondo lattice model:

$$\mathcal{H} = \mathcal{H}_f + \mathcal{H}_c + \mathcal{H}_K \quad (1)$$

Here, $\mathcal{H}_c = \sum_{\vec{k}\sigma} \epsilon_{\vec{k}} \psi_{\vec{k}\sigma}^\dagger \psi_{\vec{k}\sigma}$ describes a band of free conduction c -electrons, with a bandwidth W . For simplicity, we will consider the electron concentration, x per site, to be such that the Fermi surface of \mathcal{H}_c alone does not touch the antiferromagnetic zone boundary. $\mathcal{H}_K = \sum_i J_K \vec{S}_i \cdot \vec{s}_{c,i}$ specifies the Kondo interaction of strength J_K ; here the conduction electron spin $\vec{s}_{c,i} = \frac{1}{2} \sum_{\sigma\sigma'} \psi_{\sigma,i}^\dagger \vec{\tau}_{\sigma\sigma'} \psi_{\sigma',i}$, where $\vec{\tau}$ is the vector of Pauli matrices. Finally, $\mathcal{H}_f = \frac{1}{2} \sum_{ij} I_{ij} \vec{S}_i \cdot \vec{S}_j$ is the magnetic Hamiltonian for the spin- $\frac{1}{2}$ f -moments, \vec{S}_i , for which there is 1 per site. The strength of the exchange interactions, I_{ij} , is characterized by, say, the nearest neighbor value, I .

QNL σ M representation of the Kondo lattice: We focus on the parameter region with $J_K \ll I \ll W$. Here, it is appropriate to expand around the limit $J_K = 0$, where the local-moment and conduction-electron components are decoupled. We will consider, for simplicity, square or cubic lattices, although our results will be generally valid provided that the ground state is a collinear antiferromagnet. \mathcal{H}_f can be mapped to a quantum non-linear sigma model (QNL σ M) by standard means [14, 15]. The low-lying excitations are concentrated in the momentum space near $\vec{q} = \vec{Q}$ (the staggered magnetization) and near $\vec{q} = \vec{0}$ (the total magnetization being conserved):

$$2\vec{S}_i \rightarrow \eta_{\vec{x}} \vec{n}(\vec{x}, \tau) \sqrt{1 - \left(2a^d \vec{L}(\vec{x}, \tau)\right)^2} + 2a^d \vec{L}(\vec{x}, \tau) \quad (2)$$

where \vec{x} labels the position, $\eta_{\vec{x}} = \pm 1$ on even and odd sites, and a is the lattice constant. The linear coupling $\vec{n} \cdot \vec{s}_c$ cannot connect two points on the Fermi surface and is hence unimportant for low energy physics (such a kinematic constraint has appeared in other contexts, *e.g.* Ref. [16]); see Fig. 1b. The Kondo coupling is then replaced by an effective one, $\vec{S}_i \cdot \vec{s}_c \rightarrow a^d \vec{L} \cdot \vec{s}_c$, correspond-

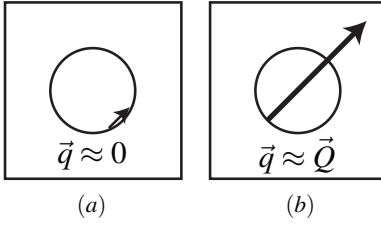


FIG. 1: With the Fermi surface (FS) of the conduction-electron component not touching the antiferromagnetic zone boundary, only the uniform component ($\vec{q} \approx 0$) of the local moments can interact with two states near the FS, as shown in (a). The linear coupling involving the staggered component, $\vec{n} \cdot \vec{s}_c$, is not kinematically favorable, as shown in (b).

ing to forward scattering for the conduction electrons; see Fig. 1a.

The mapping to the QNL σ M can now be implemented by integrating out the \vec{L} field. The effective action is

$$\begin{aligned} \mathcal{S} &= \mathcal{S}_{\text{QNL}\sigma\text{M}} + \mathcal{S}_{\text{Berry}} + \mathcal{S}_K + \mathcal{S}_c \quad (3) \\ \mathcal{S}_{\text{QNL}\sigma\text{M}} &\equiv \frac{c}{2g} \int d^d x d\tau \left[(\nabla \vec{n}(\vec{x}, \tau))^2 + \left(\frac{\partial \vec{n}(\vec{x}, \tau)}{c \partial \tau} \right)^2 \right] \\ \mathcal{S}_K &\equiv \lambda \int d^d x d\tau [\vec{s}_c(\vec{x}, \tau) \cdot \vec{\varphi}(\vec{x}, \tau)] \\ \mathcal{S}_c &\equiv \int d^d K d\varepsilon \sum_{\sigma} \psi_{\sigma}^{\dagger}(\vec{K}, i\varepsilon) (i\varepsilon - \xi_K) \psi_{\sigma}(\vec{K}, i\varepsilon) \\ &\quad + \lambda^2 \int \psi^4 \end{aligned}$$

where $\xi_K \equiv v_F(K - K_F)$. The Berry phase term for the \vec{n} field, $\mathcal{S}_{\text{Berry}}$, is not important inside the Néel phase. We have introduced a vector boson field $\vec{\varphi}$ which is shorthand for $\vec{n} \times \frac{\partial \vec{n}}{\partial \tau}$. The \vec{n} field satisfies the constraint, $\vec{n}^2 = 1$, which is solved by $\vec{n} = (\vec{\pi}, \sigma)$, where $\vec{\pi}$ labels the Goldstone magnons and $\sigma \equiv \sqrt{1 - \vec{\pi}^2}$ is the massive field. We will consider the case of a spherical Fermi surface; since only forward scattering is important, our results will apply for more complicated Fermi-surface geometries. The parameters for the QNL σ M will be considered as phenomenological [15], though they can be explicitly written in terms of the microscopic parameters. The effective Kondo coupling $\lambda = iJ_K/(4dIa^d)$.

Renormalization group analysis – tree level: We now carry out a renormalization group (RG) analysis of the effective action. We will describe the $d = 2$ case for the most part, but our conclusions remain valid for any other $d > 1$ dimensions. Our analysis involves a combination of the bosonic RG for the QNL σ M [15, 17, 18] and the fermionic RG [19]. (We note in passing that a combined bosonic/fermionic RG has been used in the context of several other problems [20, 21].) Without loss of generality, we take the ultraviolet energy cutoffs for the fermions (Λ_f) and bosons (Λ_b) to be $\Lambda \sim \Lambda_f \sim \Lambda_b$. Unless otherwise specified, the variables (\vec{q}, ω) belong to bosonic

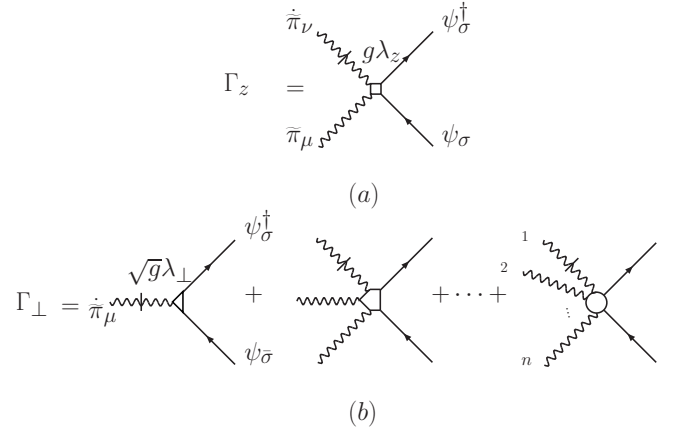


FIG. 2: The Feynman rules associate wavy lines with magnons ($\tilde{\pi}$ fields), and solid straight lines with itinerant electrons (ψ fields). A slash through a boson line indicates a time derivative (i.e. $\dot{\tilde{\pi}}$). (a) represents the four diagrams in Γ_z . (b) describes the infinite number of spin-flip vertices, Γ_{\perp} , involving an odd number of magnons.

fields, while (\vec{K}, ε) belong to fermionic fields, with \vec{K} measured from the Brillouin zone center and $k \equiv K - K_F$ is relative to the Fermi surface. Under scaling, $\omega \rightarrow s\omega$, $\varepsilon \rightarrow s\varepsilon$, $\vec{q} \rightarrow s\vec{q}$, and $k \rightarrow sk$. The fermionic kinetic term specifies [19] that $[\psi(\vec{K}, \varepsilon)] = -3/2$.

For the QNL σ M, we write $\vec{n}(\vec{x}, \tau) = [\pi_+(\vec{x}, \tau), \pi_-(\vec{x}, \tau), \sqrt{1 - \pi_+^2 - \pi_-^2}]$, and define the composite vector boson field $\vec{\varphi}$ by

$$\begin{aligned} \vec{\varphi}(\vec{x}, \tau) &\equiv \vec{n}(\vec{x}, \tau) \times \dot{\vec{n}}(\vec{x}, \tau) \\ &= \begin{pmatrix} \frac{1}{\sigma} (-\dot{\pi}_- - \dot{\pi}_+ \pi_+ \pi_- + \pi_+ \pi_+ \dot{\pi}_-) \\ \frac{1}{\sigma} (\dot{\pi}_+ + \dot{\pi}_- \pi_- \pi_+ - \pi_- \pi_- \dot{\pi}_+) \\ \dot{\pi}_- \pi_+ - \pi_- \dot{\pi}_+ \end{pmatrix} \quad (4) \end{aligned}$$

The square-root factors can be expanded, for example $\frac{1}{\sigma} = \frac{1}{\sqrt{1 - \pi_+^2 - \pi_-^2}} \approx 1 + (1/2)(\pi_+^2 + \pi_-^2) + (3/8)(\pi_+^2 + \pi_-^2)^2 + \dots$. The scaling dimensions are $[\vec{\varphi}(\vec{q}, \omega)] = 1$ and $[\vec{\varphi}(\vec{q}, \omega)] = -d$, while $[g] = 1 - d$. Note that, in order for the boson-fermion coupling term to satisfy momentum conservation, the relative angle (which does not appear in the measure) between \vec{K} and $\vec{K} + \vec{q}$ also needs to scale [20]. Based on all these, the scaling dimension of the Kondo interaction term $[d^d K d\varepsilon d^d q d\omega \psi_{\alpha}^{\dagger}(\vec{K} + \vec{q}, \varepsilon + \omega) \psi_{\beta}(\vec{K}, \omega) \vec{\varphi}(\vec{q}, \omega)]$, is $1 + 1 + d + 1 + 2(-3/2) - d = 0$. We reach the important conclusion that $[\lambda] = 0$: at the tree level, the Kondo coupling is marginal in arbitrary spatial dimensions.

Renormalization group analysis – one loop: The Kondo interaction contains longitudinal and spin-flip terms: $\mathcal{S}_K \equiv \Gamma_z + \Gamma_{\perp}$. It will be convenient to rescale the Goldstone field, $\pi = \sqrt{g} \tilde{\pi}$, and the free-field part of the QNL σ M becomes: $\mathcal{S}_{\text{QNL}\sigma\text{M}} = \frac{c}{2} \int d^d x d\tau (\partial \tilde{\pi}(\vec{x}, \tau))^2$. There are an infinite number of interaction vertices in-

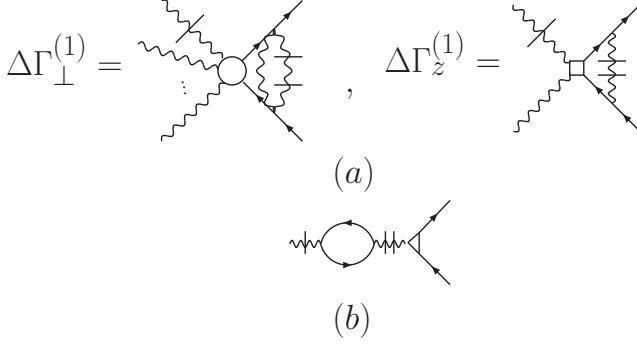


FIG. 3: (a) shows the lowest order corrections to the vertices Γ_z and Γ_{\perp} . (b) is an example of a class of diagrams that do not contribute to the beta function.

volving an increasing number of $\tilde{\pi}$ fields, always coupled to exactly two fermion fields; see Fig. 2. However, we only need to consider one representative vertex and all its loop corrections; other vertices renormalize in the same way, as dictated by symmetry [in a way similar to the case of the NL σ M itself (Ref. [18], p. 343)].

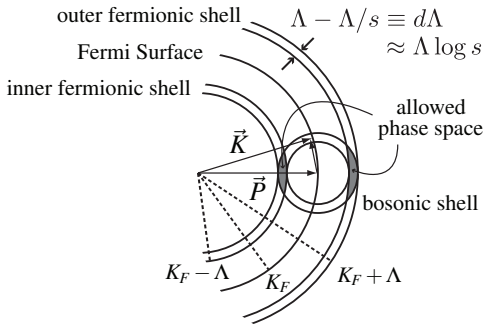


FIG. 4: Kinematics for the momentum-shell RG. Only the shaded region is integrated over.

We describe in some detail one example of a one-loop correction, that of $\Delta\Gamma_z^{(1)}$ shown in Fig. 3a. Other corrections are of a similar form, and the conclusions are the same. Summing over the Matsubara frequency leads to

$$\Delta\Gamma_z^{(1)}(\vec{q}, i\omega, \vec{P}, ip_l) = g^2 \lambda_{\perp}^2 \lambda_z i\omega \times \left(\int_{\text{inner shell}} \gamma_z^{(1)} - \frac{1}{2} \int_{\text{inner+outer shells}} \gamma_z^{(2)} \right) \quad (5)$$

where

$$\gamma_z^{(1)} = \frac{w_{P-K}^2 (-2ip_l - i\omega + \xi_K + \xi_{K+q})}{[(ip_l - \xi_K)^2 - w_{P-K}^2][(ip_l + i\omega - \xi_{K+q})^2 - w_{P-K}^2]} \quad (6)$$

$$\gamma_z^{(2)} = \frac{1}{[ip_l - w_{P-K} - \xi_K]} \frac{w_{P-K}}{[ip_l + i\omega - w_{P-K} - \xi_{K+q}]}.$$

Here, (\vec{P}, ip_l) label the energy-momentum of one of the two external fermions, while $(\vec{q}, i\omega)$ denote the energy-momentum transfer among the two external bosons (or,

equivalently, that of the two external fermions). The magnon energy is $w_{P-K} = c|\vec{P} - \vec{K}|$.

We can now consider the kinematics of these one-loop corrections. Three momenta, \vec{P} , \vec{K} , and \vec{q} , are involved in the integrals for $\Delta\Gamma_z^{(1)}$. The external-fermion momentum \vec{P} can be set to the Fermi momentum, $|\vec{P}| \approx K_F$, since any difference would be irrelevant in the RG sense. Likewise, the external-boson momentum transfer \vec{q} can be set to zero. The fermionic loop momentum, \vec{K} , is restricted to the inner and outer shells straddling the Fermi surface: $K_F + \Lambda/s < |\vec{K}| < K_F + \Lambda$ and $K_F - \Lambda < |\vec{K}| < K_F - \Lambda/s$, respectively. Finally, the bosonic momentum $\vec{P} - \vec{K}$ must be contained inside the circle defined by its cutoff Λ .

These restrictions on \vec{P} and \vec{K} lead to the construction shown in Fig. 4. The only phase space allowed by momentum conservation is the shaded region in the figure. This limits the loop integration over \vec{K} to the small angular interval from $-\Lambda/K_F$ to $+\Lambda/K_F$, and two radial shells of width $d\Lambda \equiv \Lambda - \Lambda/s \approx \Lambda \log s$ (where $s \gtrsim 1$). A simple geometric analysis shows that the allowed phase space (shaded region) is proportional to $\Lambda^2 (\log s)^{3/2}$, therefore $\Delta\Gamma_z \propto (\log s)^{3/2}$. The vertex correction is superlinear in $\log s$, so *it does not contribute to the beta function!* The Kondo coupling is still marginal at the one-loop level.

We note that if, instead of eliminating modes within the momentum shell, we integrate over the entire phase space, the vertex correction is of the order $g^2 \lambda_{\perp}^2 \lambda_z \frac{\Lambda}{K_F}$. This is consistent with the vanishing contribution to the beta function in the low-energy limit.

Finally, there are also vertex corrections due to the interactions purely among the fermion fields or purely among the QNL σ M fields. The former do not yield loop corrections in the forward-scattering channel [19]. The latter are irrelevant since g renormalizes to 0.

Renormalization group analysis – to infinite loops: The kinematic arguments so far are similar to what happens to the renormalization of the forward-scattering interactions in the pure fermion problem, where momentum conservation combined with cutoff considerations severely limit the available phase space [19]. The parallel carries over to the RG beyond one loop. We decompose the Fermi surface into $N_{\Lambda} \equiv \pi K_F / \Lambda$ patches, and rescale the momentum and energy variables for each patch in terms of Λ : $\bar{\varepsilon} = \varepsilon / \Lambda$ and so on. We also absorb a factor Λ^2 into the fermion field, so that the kinetic term for the fermions becomes $\sum_i^{N_{\Lambda}} \int d^2 k_i d\bar{\varepsilon}_i \psi_i^{\dagger} (i\bar{\varepsilon}_i - v_F \bar{k}_i) \psi_i$. Likewise, we absorb a factor $\Lambda^{5/2}$ into the $\tilde{\pi}$ field, so that the kinetic part of the QNL σ M is $\mathcal{S}_{\text{QNL}\sigma\text{M}} \sim \int d^2 q d\bar{\omega} (\bar{q}^2 + \bar{\omega}^2) \tilde{\pi}^2$. We then find that the spin-flip Kondo coupling (Γ_{\perp}) contains a factor $\Lambda^{1/2}$, and the longitudinal Kondo coupling (Γ_z) contains a factor Λ . In other words, the Kondo couplings are of the order of $(1/\sqrt{N_{\Lambda}}) \lambda_{\perp} \sum_i \int \varphi \psi^{\dagger} \psi$ and $(1/N_{\Lambda}) \lambda_z \sum_i \int \varphi \psi^{\dagger} \psi$, respectively. These extra $1/\sqrt{N_{\Lambda}}$

and $1/N_\Lambda$ factors make their contributions negligible to infinite loops, except for a chain of particle-hole bubbles (in the spin-flip channel), the lowest order of which is shown in Fig. 3b. The latter does not contribute to the beta function, since the two conduction electron poles are located on the same side of the real axis [19].

The Kondo coupling is therefore marginal to infinite loops. This contrasts to what happens in the single-impurity Kondo problem. There, the Kondo coupling is relevant, and flows to infinity, which signifies singlet formation in the ground state and a concomitant Kondo resonance in the excitation spectrum. In the paramagnetic phase of the Kondo lattice, the Kondo coupling is believed to flow to a related strong coupling fixed point where, again, Kondo resonances are generated and the Fermi surface becomes large.

In our case, a marginal Kondo coupling implies that there is no Kondo singlet formation and the Fermi surface will stay small in the sense defined earlier.

Large N limit: To see explicitly the small Fermi surface, we turn to a large N generalization (this is different from the previous N_Λ) of the effective action [22]. The $N \rightarrow \infty$ limit is taken with the spin symmetry of the conduction electrons enlarged from $SU(2)$ to $SU(N)$, and the symmetry of the magnons from $O(2)$ to $O(N^2-2)$. The effective Kondo coupling is rescaled to λ/\sqrt{N} . Leaving details for elsewhere [22], we quote the equation for the conduction-electron self-energy, $\Sigma(\vec{K}, \tau) = \int d\vec{q} \lambda^2 G_{\varphi,0}(\vec{q}, -\tau) G(\vec{K} + \vec{q}, \tau)$, where $G_{\varphi,0}(\vec{q}, -\tau) = \langle T_\tau \tilde{\pi}(\vec{q}, -\tau) \tilde{\pi}(\vec{q}, 0) \rangle_{QNL\sigma M}$, and $G(\vec{K}, \tau) = -\langle T_\tau c(\vec{K}, \tau) c^\dagger(\vec{K}, 0) \rangle$ is the full conduction-electron propagator. We find that $\Sigma(\vec{K}, \omega) = a\omega - ib|\omega|^{d_{\text{sgn}}}\omega$, where a, b are constants whose dependence on λ has the first non-vanishing term $\sim \lambda^2$. (When the four-fermion interaction among the ψ 's is included, there will be an ω^2 term added to $\text{Im}\Sigma$.) It follows from $G(\vec{K}, \omega) = [\omega - \xi_{\vec{K}} - \Sigma(\vec{K}, \omega)]^{-1}$ that the Fermi surface is the same as that of the conduction-electron component alone. The Fermi surface is indeed small.

We now turn from the asymptotically exact results to their implications. It is well accepted that two other phases specified earlier occur in the zero-temperature phase diagram of the Kondo lattice: a paramagnetic phase with a large Fermi surface, PM_L , and an antiferromagnetic one with a larger Fermi surface, AF_L . The existence of PM_L has been most explicitly seen in the large- N limit of the $SU(N)$ generalization of the model [23, 24] [where $\Sigma(\vec{K}, \omega) = (v^*)^2/(\omega - \epsilon_f^*)$ contains a pole and, correspondingly, $G(\vec{K}, \omega)$ yields a large Fermi surface]. Our results here demonstrate that the antiferromagnetic part of the phase diagram in principle accommodates a genuine phase transition from AF_S to AF_L . For commensurate antiferromagnetic ordering (and to order Δ/W in

the incommensurate case, where Δ is the SDW gap of the AF_L phase), this corresponds to a Lifshitz transition with a change of Fermi surface topology. Such a transition has been heuristically discussed in the past [7, 9]; our exact result on the stability of the AF_S phase provides evidence for the existence of this Lifshitz transition.

In addition, the existence of the AF_S phase opens the possibility for a direct quantum transition from the AF_S to the PM_L phases. For this transition to be continuous, the quasiparticle residues z_S and z_L must vanish when the QCP is approached from the two respective sides. The quantum critical point is then a non-Fermi liquid with a divergent effective mass; local quantum criticality [6, 7] is one such example. The results reported here, therefore, provide a new perspective to view the local quantum criticality.

Acknowledgments: We thank R. Shankar for an instructive discussion on the fermionic RG, E. Abrahams, C. Bolech, A. V. Chubukov, E. Fradkin, S. Kirchner, A. Ludwig, A. Rosch, S. Sachdev, T. Senthil and F. Steglich for useful discussions, NSF, the Robert A. Welch Foundation and the W. M. Keck Foundation for partial support, and KITP, ACP, and the Lorentz Center for hospitality.

-
- [1] G. R. Stewart, *Rev. Mod. Phys.* **73**, 797 (2001).
 - [2] H. v. Löhneysen *et al.* (2006), cond-mat/0606317.
 - [3] J. A. Hertz, *Phys. Rev. B* **14**, 1165 (1976).
 - [4] A. J. Millis, *Phys. Rev. B* **48**, 7183 (1993).
 - [5] T. Moriya, *Spin Fluctuations in Itinerant Electron Magnetism* (Springer-Verlag, 1985).
 - [6] Q. Si *et al.*, *Nature* **413**, 804 (2001).
 - [7] Q. Si *et al.*, *Phys. Rev. B* **68**, 115103 (2003).
 - [8] P. Coleman *et al.*, *J. Phys.: Condens. Matter* **13**, R723 (2001).
 - [9] T. Senthil *et al.*, *Phys. Rev. B* **69**, 035111 (2004).
 - [10] Y. Ōnuki *et al.*, *Acta Phys. Pol. B* **34**, 667 (2003).
 - [11] A. McCollam *et al.*, *Physica B* **359**, 1 (2005).
 - [12] S. Paschen *et al.*, *Nature* **432**, 881 (2004).
 - [13] H. Shishido *et al.*, *J. Phys. Soc. Jpn.* **74**, 1103 (2005).
 - [14] F. D. M. Haldane, *Phys. Rev. Lett.* **50**, 1153 (1983).
 - [15] S. Chakravarty *et al.*, *Phys. Rev. B* **39**, 2344 (1989).
 - [16] S. Sachdev *et al.*, *Phys. Rev. B* **51**, 14874 (1995).
 - [17] D. R. Nelson and R. A. Pelcovitz, *Phys. Rev. B* **16**, 2191 (1977).
 - [18] P.M. Chaikin and T.C. Lubensky, *Principles of Condensed Matter Physics* (Cambridge U. Press, 1995).
 - [19] R. Shankar, *Rev. Mod. Phys.* **66**, 129 (1994).
 - [20] C. Pépin *et al.*, *Phys. Rev. B* **69**, 172401 (2004).
 - [21] S. W. Tsai *et al.*, *Phys. Rev. B* **72**, 054531 (2005).
 - [22] S. J. Yamamoto and Q. Si, (unpublished).
 - [23] A. Auerbach and K. Levin, *Phys. Rev. Lett.* **57**, 887 (1986).
 - [24] A. J. Millis and P. A. Lee, *Phys. Rev. B* **35**, 3394 (1987).